Journal of Inflammation Research

Dovepress
Taylor & Francis Group

Open Access Full Text Article

ORIGINAL RESEARCH

Fatty Acid Transporter CD36 Promotes Ox-LDL-Induced Senescence of Vascular Endothelial Cells in Preeclampsia

Yanxuan Xiao[1,2,*], Maliang Tao[3,*], Yiqi Yu[1,*], Ruiyan Bai[1,2], Yunting Zhuang[1,2], Qiuyu Huang[1], Jiexing He[1], Zeshan Lin[1,2], Mingze Gao[1], Jiaqi Li[1], Yuting Wang[1], Yao Xu[1], Xinyang Shen[1], Zhenqin Huang[1], Yuan Yao[1], Zhiyong Chen[1], Qian Chen[1], Zhijian Wang[1,4]

[1]Department of Obstetrics and Gynecology, Nanfang Hospital, Southern Medical University, Guangzhou, 510515, People's Republic of China; [2]School of Nursing, Southern Medical University, Guangzhou, 510515, People's Republic of China; [3]Department of Laboratory Medicine, Nanfang Hospital, Southern Medical University, Guangzhou, 510515, People's Republic of China; [4]Department of Obstetrics and Gynecology, Guangdong Provincial Key Laboratory of Major Obstetric Diseases, Guangdong Provincial Clinical Research Center for Obstetrics and Gynecology, Guangdong-Hong Kong-Macao Greater Bay Area Higher Education Joint Laboratory of Maternal-Fetal Medicine, The Third Affiliated Hospital, Guangzhou Medical University, Guangzhou, 510150, People's Republic of China

*These authors contributed equally to this work

Correspondence: Qian Chen; Zhijian Wang, Department of Obstetrics and Gynecology, Nanfang Hospital, Southern Medical University, Guangzhou, 510515, People's Republic of China, Email chenqianqian430@qq.com; wzjnfyy@163.com

Purpose: To elucidate the association between CD36 expression and senescence induced by oxidized low-density lipoprotein (ox-LDL) in patients with preeclampsia (PE).

Patients and Methods: We conducted a gene set enrichment analysis on RNA-sequencing data of placentas, focusing on CD36, a key gene in lipid metabolism. CD36 and ox-LDL expression were measured via qRT-PCR, Western blotting, immunohistochemistry, and immunofluorescence. We used plasmid and siRNA transfection to modulate CD36 expression in human umbilical vein endothelial cells, exposing them to ox-LDL to assess cellular senescence, oxidative stress, and angiogenesis. A co-culture system was constructed to examine how endothelial cell senescence affects trophoblast migration and invasion.

Results: In patients with PE, CD36 expression significantly increased in the vascular endothelial cells of the placenta. An association was observed between elevated CD36 and ox-LDL-induced cell senescence, accompanied by intracellular oxidative stress, endothelial cell angiogenesis disorders, and decreased trophoblast function in the placenta.

Conclusion: Our study has initially identified significant alterations in CD36 expression in PE placentas, which may be one of the driving factors for the occurrence of senescence. Further research is warranted to explore the mechanism between CD36 and PE-related placental senescence, which may offer novel avenues for the diagnosis and treatment of PE.

Keywords: placenta, preeclampsia, CD36, placental senescence, endothelial injury

Introduction

Preeclampsia (PE) is a life-threatening pregnancy complication characterized by new-onset hypertension, proteinuria, and organ damage after 20 weeks of gestation.[1,2] It impacts 2% to 5% of all pregnancies and leads to adverse perinatal outcomes, including cardiovascular complications, renal dysfunction, and limited fetal growth.[3,4] The causative factors of PE are thought to be multifaceted, encompassing oxidative stress, atypical immune system activation, and inflammation.[5] However, underlying mechanisms contributing to the pathophysiology of PE are still poorly understood. Exploring the mechanisms of PE is vitally important for maternal and infant health.

Cell senescence refers to irreversible and permanent cell cycle arrest.[6] Physiological placental aging is beneficial to the normal development of the placenta.[7] However, some abnormal conditions, such as oxidative stress, can lead to premature aging of the placenta.[8] Studies have shown that women with PE experience accelerated epigenetic aging

Received: 10 June 2025
Accepted: 9 September 2025
Published: 16 September 2025

during pregnancy.[9,10] Increased cell senescence can be observed in PE blood, fat, and placental tissues.[10,11] However, more studies have suggested that the aging state of PE patients was derived from the placenta.[11,12] Under the influence of multiple factors, the cell senescence of the placenta accelerated, and senescence-associated secretory phenotype (SASP) was then produced by the placenta and released into the blood circulation or other organs. Therefore, exploring abnormal aging of the placenta is essential for understanding the pathogenesis of PE.

CD36, known as Fatty Acid Translocase (FAT), is crucial in multiple biological processes. It is responsible for the uptake of lipids, transport of fatty acids, regulation of inflammatory responses, and modulation of immune cell activities. As a gene related to lipid metabolism, CD36 has been proven to be associated with various metabolic disorders, such as obesity, metabolic syndrome, and cardiovascular diseases.[13] CD36 facilitates inflammation by inducing ferroptosis in macrophages in the context of obesity-associated severe acute pancreatitis.[14] Conversely, the absence of CD36 mitigates diabetic kidney disease by reinstating fatty acid oxidation and enhancing mitochondrial function.[15] S-palmitoylation of CD36 augments lipid uptake in macrophages,[16] whereas S-nitrosylation acts as a protective mechanism against lipid-induced endothelial toxicity.[17] However, its specific role in the onset of PE remains unclear. Interestingly, aging phenotypes caused by abnormal fatty acid metabolism have been reported.[18] A study published in Nature also reported that CD36 is a potential target for regulating cell senescence.[19] These studies suggest a possible relationship between CD36, abnormal fatty acid metabolism, and placental aging of PE.

Our study was centered on the exploration of pathways and genes associated with lipid metabolism. By conducting a more in-depth analysis of RNA-seq data, we observed a significant upregulation of CD36 in the endothelial cells of the PE placenta. This upregulation was found to be associated with an enhanced damaging effect of ox-LDL on the placenta. Therefore, we designed and carried out a series of experiments to better understand the underlying mechanisms.

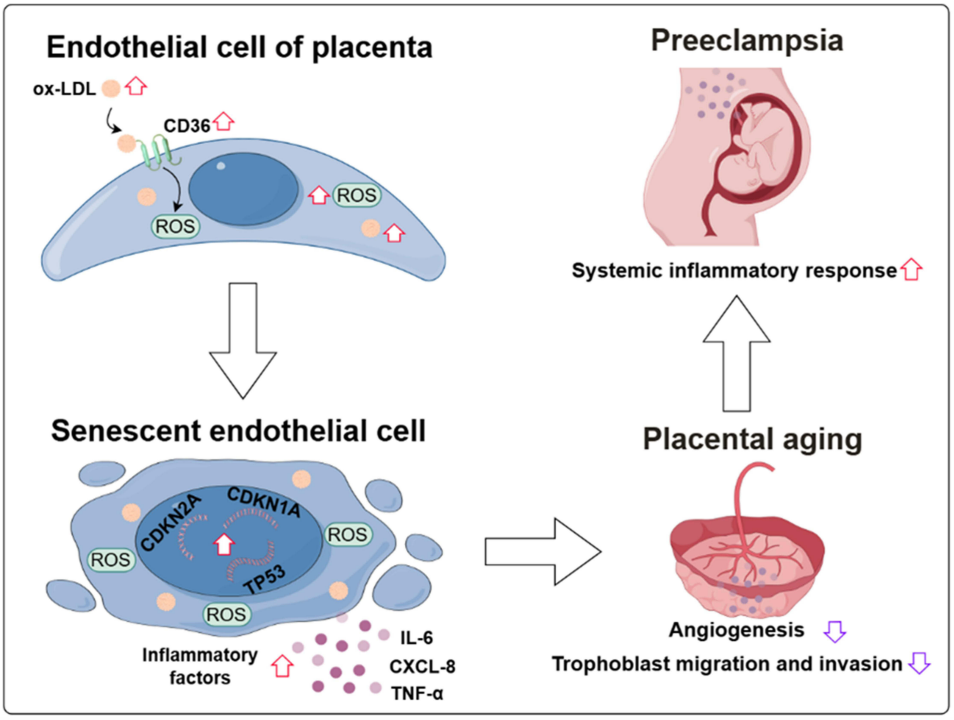

Scheme 1 Schematic for explaining the potential role of CD36 in PE (By Figdraw). Elevated CD36 in PE placental vascular endothelial cells leads to ox-LDL accumulation, oxidative stress, and cell senescence, impairing vascular function. Senescent endothelial cells release inflammatory factors, which locally hinder trophoblast cell migration and invasion and can also enter the bloodstream, causing systemic inflammation in PE patients.

Material and Methods

Plasma and Placental Samples

The present study received approval from the Research Ethics Committee of Nanfang Hospital, Southern Medical University (NFEC-201601-K1-05). Between June 2021 and December 2022, a total of 38 plasma and placental samples were collected from the Department of Obstetrics and Gynecology at Nanfang Hospital. The inclusion criteria for the study subjects were based on the diagnostic criteria for PE established by the International Society for the Study of Hypertension in Pregnancy (ISSHP).[20] NC samples were collected from full-term pregnant women who delivered by cesarean section due to abnormal fetal position or poor pelvic condition. The peripheral blood samples of pregnant women were all collected within one week prior to delivery. After collecting blood in tubes with EDTA, centrifuged the samples at 3000 × rpm for 30 minutes at 4 °C to obtain plasma. Then, store them at −80 °C for ELISA experiments. Four distinct locations of the placenta were collected within 30 minutes after delivery from the intermediate part between the chorionic villi and the maternal basal surface. Afterward, the tissue was washed in PBS buffer and stored in RNAlater at −80 °C for subsequent experiments. Clinical information of the samples and comparison between groups were listed in Table S1.

Gene Set Enrichment Analysis (GSEA) of Transcriptome Sequencing Data

The data we explored came from the transcriptome sequencing dataset of our research group's previous study,[21] in which we conducted analysis on all samples. We used the GSEA tool (https://www.gsea-msigdb.org/gsea) for gene set enrichment analysis. In confirming PE placental Aging by GSEA analysis, aging-related genes were collected from the Aging Atlas database (https://ngdc.cncb.ac.cn/aging), GenAge database (https://genomics.senescence.info/genes) and the "SAUL_SEN_MAYO" gene set from the GSEA database (https://www.gsea-msigdb.org/gsea/msigdb/mouse/geneset/SAUL_SEN_MAYO). The enrichment level was determined by calculating the Normalized Enrichment Score. Enrichment results with a p-value of <0.05 and a false discovery rate (FDR) of <0.25 were considered to be significantly enriched.

GO and KEGG Analysis of Lipid-Related Differentially Expressed Genes

We collected all lipid metabolism-related genes from the MSigDB and identified the intersection of genes with differentially expressed genes. The KEGG database (http://www.genome.jp/kegg/) and GO database (http://www.geneontology.org/) were used to determine the pathways and biological functions associated with the intersecting genes. Enriched GO and KEGG terms with a p-value of <0.05 were considered statistically significant.

Senescence Marker Selection

CDKN2A, CDKN1A, and TP53 were selected as senescence biomarkers after systematic literature review because they constitute canonical cell-cycle inhibitors widely recognized as core senescence markers.[22,23] The CDKN2A pathway and the CDKN1A/TP53 axis independently regulate cell-cycle arrest while responding to diverse pro-senescent stimuli, including oxidative stress and telomere attrition through coordinated DNA-damage responses.[24,25] Fine-tuning these pathways balances organismal healthspan with tumor suppression yet can also promote accelerated aging.[26] Cellular senescence generally causes the activation of some paracrine effects. Prominent among these are inflammatory mediators, including IL-6, CXCL-8, and TNF-α, commonly elevated when senescence occurs.[27] Consequently, we simultaneously profiled these SASP mediators to delineate the secretory signature accompanying placental endothelial senescence. Although senescence-associated heterochromatin foci (SAHF) formation and γ-H2AX foci are established senescence indicators, SAHF depends on CDKN2A or TP53 signaling already interrogated, whereas γ-H2AX marks DNA damage but lacks senescence specificity.[28,29] Therefore, they were not assayed concurrently in this study.

RNA Extraction and Real-Time Fluorescent Quantitative PCR

Total RNA extraction was carried out using Trizol (Invitrogen, USA). For gene expression quantification, reverse transcription and qRT-PCR were performed on the LightCycler 480 system (Roche, Switzerland) using the HiScript Reverse Transcription Kit and ChamQ SYBR Green qPCR Kit (Vazyme, China) following the manufacturer's

instructions. The $2^{-\Delta\Delta CT}$ method was employed, with ACTB serving as the internal control for normalization and fold change calculation. Table S2 lists the primer sequences used in the qRT-PCR.

Western Blot

After obtaining placental tissue or cell masses, total protein was extracted using RIPA lysis buffer. The BCA assay kit (Beyotime, China) was utilized to ascertain the content of protein. Proteins were separated using 12% SDS-PAGE gel electrophoresis and then transferred to PVDF membranes with 0.45 μm pore size. After blocking with 5% BSA and washing with TBST, the membrane was incubated overnight with the diluted primary antibody, including CD36 (1:1000, 18836-1-AP, Proteintech, China), ox-LDL (1:3000, PAA527Hu08, Cloud-Clone, China), CDKN2A (1:4000, 10883-1-AP, Proteintech, China), CDKN1A (1:2000, 10355-1-AP, Proteintech, China), TP53 (1:20,000, 10442-1-AP, Proteintech, China). The next day, the membrane was incubated for 2 hours at room temperature with HRP secondary antibody (1:20000, bs-0295G-HRP, Bioss, China) after washing with TBST. The membrane was washed with TBST again, then ECL luminescent solution (Beyotime, China) was added, and the gel imaging system (Biolight, China) was used to photograph the membrane, which was then quantified with Image J.

Immunohistochemistry

As soon as the placental samples were fixed in 4% paraformaldehyde (Rarbio, China), they were treated with xylene and alcohol. The tissue pieces were then treated with citrate antigen retrieval buffer after being microwaved. After three PBS washes, the tissue slides were incubated in 3% hydrogen peroxide for 20 minutes, followed by one hour at room temperature in 3% BSA. CD36 antibody (1:600, 18836-1-AP, Proteintech, China) or ox-LDL (1:100, PAA527Hu08, Cloud-Clone, China) was applied to the sections and incubated overnight at 4°C. We then added goat anti-rabbit secondary antibody (1:2000, ab205718, Abcam, UK) to the samples and incubated them at room temperature for an hour before counterstaining them with hematoxylin for five minutes. Then treating the slides with diaminobenzidine for two minutes. The negative control had the same experimental conditions as the experimental group except that no target antibody was added. All the slides were observed and photographed under a microscope (Olympus, Japan). Three images were taken of each tissue. The staining intensity was analyzed using ImageJ (ImageJ Software Inc., USA), and the analysis result was the average AOD value (average optical density) of the three regions of each image.

Enzyme-Linked Immunosorbent Assay

ELISA kits (Meimian, China) were utilized to measure the concentrations of sCD36, ox-LDL, IL-6, CXCL-8, and TNF-α in tissues or plasma. Thoroughly mix reagents and prepare standard, blank, and sample wells. Dilute the standard in a gradient, then add 50 μL of both the standard and sample to the appropriate wells. Cover, gently shake, and incubate at 37 °C for 30 minutes. Discard the liquid, wash wells with washing solution, shake for 30 seconds, discard, and dry with absorbent paper. Repeat washing 5 times. Add 50 μL of HRP enzyme-labeled reagent to each well, shake, and incubate at 37 °C for 30 minutes. Remove liquid, wash wells, shake, discard, and dry with absorbent paper, repeating 5 times. Add 50 μL of chromogenic solutions A and B to each well, shake gently, and incubate at 37 °C for 10 minutes in the dark. Finally, add 50 μL of stop solution. Measure the OD values of each well at a wavelength of 450 nm (SpectraMax I3x, USA). The standard curve was drawn by the four-parameter logistic curve method in ELISACalc. Determine the concentration level based on the OD value of the sample.

Immunofluorescence

Placental samples or cells were fixed in 4% paraformaldehyde (Rarbio, China), followed by treatment with xylene and ethanol. Tissue sections were then incubated in citrate antigen retrieval buffer and heated using a microwave oven. After three washes with TBST, the tissue slides were exposed to 3% H_2O_2 for 20 minutes. Subsequently, the sections were soaked in 3% BSA at room temperature for 1 hour. The CD36 antibody (1:1000, 18836-1-AP, Proteintech, China) or β-galactosidase antibody (1:400, bs-4960R, Bioss, China) was incubated overnight at 4°C. After washing the sections with TBST, the secondary antibody (1:4000, Abcam, ab205718, UK) was applied and incubated for 1 hour in a dark room. Following that, the sections were incubated with iFluor® 488 tyramide working solution (AAT Bioquest, USA) for 10 minutes at room temperature. The sections were then repeatedly washed with TBST and wash buffer (Biossci, China).

The same process was repeated for incubation with ox-LDL antibody (1:50, PAA527Hu08, Cloud-Clone, China) and secondary antibody (1:600, Life Technologies, A32754, USA). Finally, the cells were stained with DAPI (Solarbio, China) and the slides were mounted with a fluorescence mounting medium (Southern Biotech, USA). Image acquisition and analysis were performed using a microscope (Olympus, Japan). Two images were taken of each tissue. The staining intensity was analyzed using ImageJ (ImageJ Software Inc., USA), and the analysis result was the average IOD value (integrated optical density) of the three regions of each image.

Cell Culture

HUVECs and HTR8/SVneo from the American Type Culture Collection (ATCC, USA) were cultured in DMEM and 1640 medium (Gibco, USA) with 10% fetal bovine serum (Gibco, USA). The cells were maintained in 5% CO_2 humidified atmospheres at 37°C.

Cell Transfection

We obtained the plasmids pcDNA3.1, pcDNA-3.1-CD36, si-control and si-RNA from Genechem (China). Following the manufacturer's instructions, Lipofectamine 3000 (Invitrogen, USA) was used for transfection. HUVECs transfected with the plasmids and si-RNA were collected 48 hours later for further experiments. The specific si-RNA sequences can be found in Table S2.

Cellular Intervention with Ox-LDL

Following transfection, at 8 hours, the HUVECs were treated with ox-LDL (Yiyuan biotechnology, China) at a concentration of 150 μg/mL for 24 hours, as reported in the literature. This treatment was performed for subsequent functional assays.[30]

CCK-8 Cell Proliferation Assay

Following the digestion and re-suspension of HUVECs, a cell suspension concentration of 20,000 cells/mL was prepared. Subsequently, 100 μL of this cell suspension was aliquoted into each well of a 96-well plate. After allowing for cell adhesion, the cells were subjected to ox-LDL interventions at concentrations of 0, 50, 100, 150, and 200 μg/mL. Additionally, 10% CCK-8 detection reagent was added at time points of 0, 12, 24, 36, and 48 hours. Post a 1-hour incubation period, the absorbance at 450 nm was measured (SpectraMax I3x, USA), and the cell proliferation rate was subsequently analyzed.

Intracellular ROS Level Determination

The day before the assay, cells were plated to ensure a confluency of 50% at the time of measurement. DCFH-DA (Beyotime, China) stock solution was diluted to a working concentration of 10 μM with PBS. On the following day, the cell culture supernatant was removed, and 500 μL of the working solution was added to cover the cells. The cells were then incubated at 37°C in a light-protected cell culture incubator for 30 minutes. Afterward, the cells were washed with PBS and observed and photographed using a confocal microscope (Zeiss LSM 780, Germany).

Angiogenesis Assay

HUVECs were seeded on diluted basement membrane matrix (Corning, USA) at an equal cell density. Each group of cells was seeded in triplicate. After 4 hours of cell seeding, the tube-forming ability was observed. Image J software (National Institutes of Health, USA) was used to analyze the number of tubes, tube length, and branching points in each group to reflect the angiogenic potential.

Cell Scratch Assay

HTR8/SVneo cells were seeded into a 6-well plate at a density of 1.5 million cells per well for the cell scratch assay. Upon reaching 90% confluence, a scratch was introduced using a 1 mL pipette tip. Subsequently, the cells were washed three times with PBS and cultured in different HUVECs culture supernatants. Images were captured at 0 hours and 24

hours post-scratch using an Olympus microscope (Japan). The collected data were analyzed with ImageJ software (National Institutes of Health, USA).

Cell Invasion Assay

HUVECs with different treatment were cultured at the bottom of a 24-well plate, while normal HTR8/SVneo cells were cultured in the transwell insert. Following a 24-hour co-culture period, the transwell chamber was fixed with 4% paraformaldehyde (Rarbio, China) for 20 minutes. Post-fixation, the solution was discarded, and the cells were washed once with phosphate-buffered saline (PBS). Subsequently, the cells were stained with crystal violet (Beyotime, China) for 20 minutes and then washed three times with PBS. Residual stromal cells and non-invasive cells in the chamber were gently removed using a cotton swab. Observe the cells under a microscope (Olympus, Japan) and capture images. Subsequently, the quantity of invaded cells is determined with the Cell Counter Plugin within ImageJ (National Institutes of Health, USA). The number of crystal violet-staining cells reflected the ability of cell invasion.

Data Analysis

All statistical analyses of the study were performed using SPSS 21.0 (IBM SPSS 21.0, USA). Data were presented as mean ± standard deviation (SD) from at least three independent experiments. Continuous variables were compared between groups using Student's *t*-test or paired *t*-test, while categorical variables were compared using the chi-square test. Correlation analysis was conducted using Pearson or Spearman analysis based on the variable types. $P < 0.05$ was considered statistically significant.

Limitations

A key limitation of this study is the small sample size employed across experiments. Tissue degradation during isolation or storage, outlier exclusion and limited biopsy availability for multiplex testing all reduced final numbers. Although we provided a complete traceability matrix detailing sample allocation rationale, which documenting every exclusion reason and inter-assay overlap, the small sample size used for critical senescence markers inevitably constrain generalizability of our findings (Table S3). Future investigations using larger cohorts coupled with standardized tissue-allocation protocols are necessary to confirm the robustness of senescence in PE pathogenesis.

Results

The Lipid Metabolism of the Placenta in PE is Abnormal, and CD36 Was the Key Upregulated Gene

Previously, 65 high-quality placenta samples were applied for transcriptome sequencing, including 33 from PE patients and 32 from normal pregnant women.[21] To explore the potential pathogenesis of PE, Gene Set Enrichment Analysis (GSEA) was conducted. The results revealed the enrichment of upregulated pathways including signaling pathways such as the ribosome, cytokine-cytokine receptor interaction, antigen processing and presentation, and several others (Figure 1A and Table S4). The top three pathways have been proven to participate in protein synthesis, immune regulation, and antigen presentation, maintaining cellular function and immune system balance, which may be associated with the pathogenesis of PE. In contrast, downregulated pathways showed enrichment primarily in steroid hormone biosynthesis and the metabolism of xenobiotics by cytochrome P450, which is mainly responsible for hormone synthesis and drug metabolism. Interestingly, we found that the adipocytokine and peroxisome proliferators-activated receptors (PPAR) signaling pathways are involved in lipid metabolism among the upregulated pathways. They are crucial for maintaining energy balance and metabolic health, and their dysregulation could lead to various metabolic diseases, including obesity, diabetes, and cardiovascular diseases.

To understand the enrichment of lipid-related genes in differentially expressed genes, we collected the lipid-related genes from the Molecular Signatures Database. After overlapping these genes with our differentially expressed genes, we obtained 53 overlapping genes (Table S5 and Figure S1A). To confirm the specific function of these lipid-related differentially expressed genes, we performed further enrichment analysis. Gene Ontology (GO) analysis revealed that

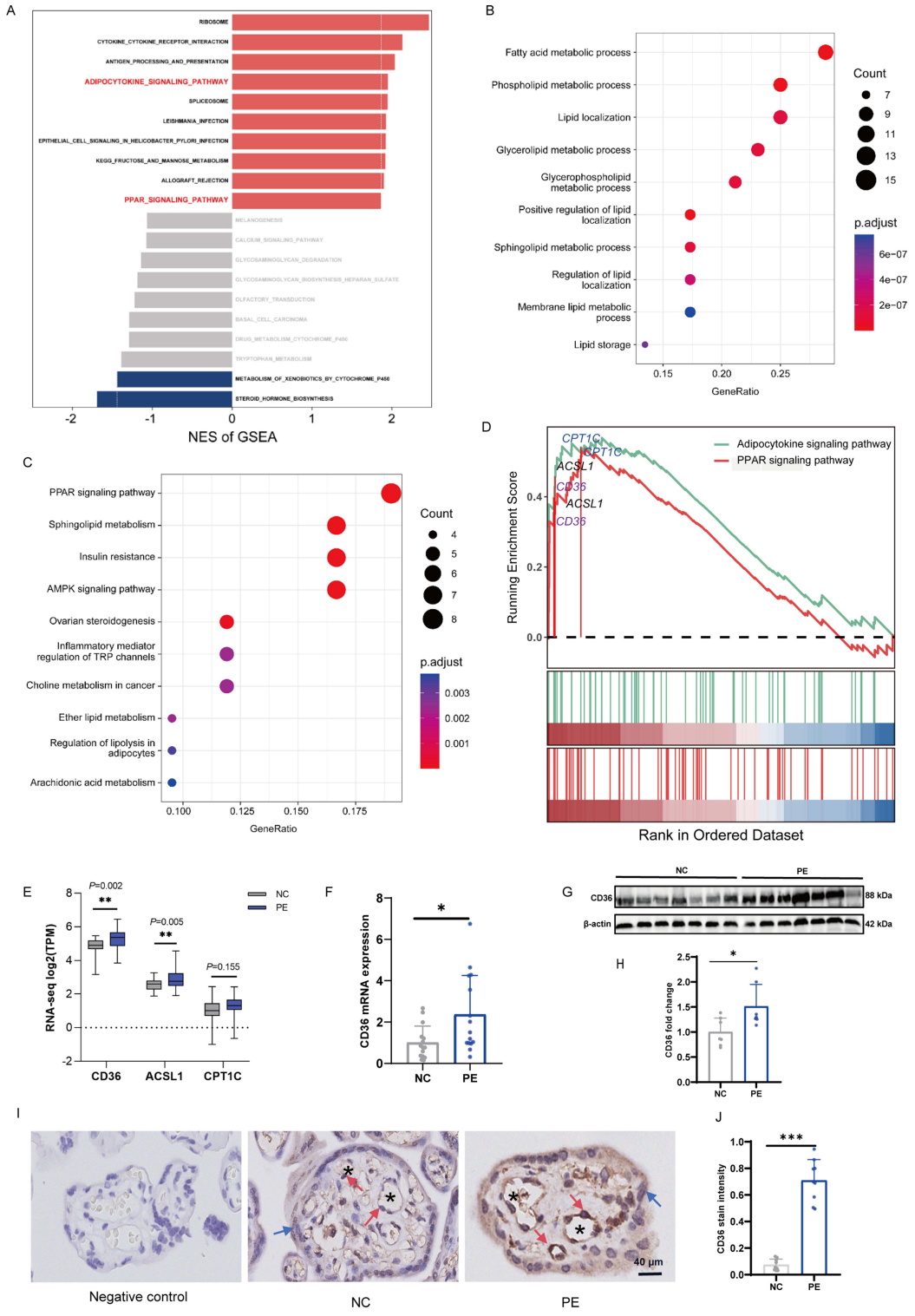

Figure 1 The lipid metabolism of the placenta in PE is abnormal, and CD36 is a key upregulated gene. (**A**) Bar graph showing results of the top 10 (top) or bottom 10 (bottom) pathways in GSEA. All cascades, except gray, were significantly enriched ($P < 0.05$). (**B**) GO enrichment analysis results of 53 cross genes. (**C**) KEGG enrichment analysis results of 53 cross genes. (**D**) GSEA plot showing the common core genes in two pathways (P-value < 0.05, FDR q-value < 0.25). (**E**) Boxplot of CD36, ACSL1, CPT1C mRNA expression in PE placentas (n = 33) compared with normal placentas (n = 32); unpaired *t* test. (**F**) CD36 mRNA expression in the external PE placentas (n = 15) compared with normal placentas (n = 15); unpaired *t* test. (**G** and **H**) The protein expression of CD36 (**G**) and quantitative results in the PE placentas (n = 7) compared with normal placentas (n = 7) (H); unpaired *t* test. (**I** and **J**) Immunohistochemical localization of the CD36 (*shows the vascular lumen in the villi; red arrows show vascular endothelial cells, which line the inner wall of the blood vessels and are flat and arranged in a single layer; blue arrows show syncytiotrophoblast, differentiated from cytotrophoblast cells, with large nucleus and nuclear fusion) (**I**) and quantitative results in the PE group (n=3) and NC group (n=3) (J); unpaired *t* test. The data are shown as the mean ± SD of three independent experiments; *p < 0.05, **p < 0.01, ***p < 0.001.

https://doi.org/10.2147/JIR.S538337

these lipid-related differentially expressed genes were significantly involved in fatty acid metabolism, lipid localization, and lipid storage processes (Figure 1B). Kyoto Encyclopedia of Genes and Genomes (KEGG) enrichment analysis showed that these genes were related to PPAR, phospholipid metabolism, and insulin resistance pathways (Figure 1C). These results indicated that dysregulated lipid metabolism may function in the pathogenesis of the PE.

To evaluate the enrichment of the differentially expressed gene set within the complete signaling pathways, we calculated the normalized enrichment score (NES). The results demonstrated a notable NES of 1.95 ($P < 0.001$) for the adipocytokine signaling pathway and 1.87 ($P < 0.001$) for the PPAR signaling pathway. From the core genes of these two pathways, we identified three key overlapping genes - CD36, ACSL1, and CPT1C (Figure 1D and Figure S1B). Importantly, CD36, Acyl - CoA Synthetase Long-Chain Family Member 1 (ACSL1), and Carnitine Palmitoyltransferase 1C (CPT1C) were positioned before the peak of the enrichment curve, underscoring their significance in these pathways (Figure 1D). Subsequently, we compared the expression differences of these three genes in the sequencing results. We found that all of them expressed higher in the PE group than in the NC group, with the expression difference of CD36 being the most pronounced ($P = 0.002$) (Figure 1E).

To investigate the relationship between CD36 expression and clinical outcomes, we classified all pregnant women into a high CD36 expression group and a low CD36 expression group according to the median value of mRNA expression. We compared the occurrence of early-onset PE, severe PE, fetal growth restriction, low birth weight infants, and the male neonate rate between the two groups of PE patients. In the high CD36 expression group, there was a significant increase in the proportion of fetal growth restriction, low birth weight infants, and male fetuses ($P < 0.05$) (Table S6). This suggested that the expression level of CD36 in PE patients was meaningful for understanding specific clinical outcomes. However, we did not observe any difference in CD36 expression levels between PE subtypes (Table S6).

Abnormal expression of CD36 frequently occurs in obese individuals, contributing to higher levels of energy metabolism and weight gain. Thus, we speculated that the differential expression of CD36 in the placenta may be attributed to differences in patient weight. We compared the value of body mass index (BMI) in pregnant women. We found PE patients showed a more dispersed BMI distribution, with a higher proportion of both high and low BMI (Figure S2A and B). However, when comparing the two groups as a whole, there was no statistically significant difference ($P > 0.05$) (Figure S2B). The correlation between CD36 expression and BMI has no significance as well ($P > 0.05$) (Figure S2C). We then categorized the pregnant women into normal control (NC), simple obesity (NCOB), simple PE (PE), and PE with obesity (PEOB) based on BMI. We observed that CD36 expression increased in PE patients regardless of obesity status (Figure S2D). Furthermore, after matching for BMI, the expression of CD36 in the PE group was significantly higher than the NC group ($P < 0.01$) (Figure S2E). According to aforementioned findings, it can be considered that the association between CD36 expression and obesity may not be statistically significant in the PE population. However, it was observed that CD36 expression was closely linked to the presence of PE.

To validate the results of our sequencing data, we further tested the mRNA expression of CD36 in other non-sequenced samples, and these samples were simply divided into normal and PE groups according to the available analysis results. Our findings indicated that CD36 expression was elevated in the PE group with significant individual variability, which was consistent with the sequencing results (Figure 1F). We unveiled elevated protein levels of CD36 in the placenta using Western blot (Figure 1G and H). Preliminary immunohistochemical results showed the localization of CD36 in the syncytiotrophoblast and vascular endothelium, with heightened expression observed in the PE placenta (Figure 1I and J).

Ox-LDL and CD36 Were Significantly Colocalized in the PE Placentas

CD36 functions as a fatty acid transport protein, facilitating the cellular uptake of extracellular free fatty acids for storage and utilization, thereby contributing to the maintenance of lipid metabolism balance. Considering that ox-LDL is a molecule that closely associated with vascular injury, and most of it can be transported through CD36, we formulated the hypothesis that CD36 may play a role in the placental dysfunction induced by ox-LDL. Consequently, we compared the ox-LDL expression in the placenta between the two groups. The PE placenta showed a significantly higher level of ox-LDL (Figure 2A–C). Preliminary immunostaining images showed ox-LDL predominantly within placental vascular endothelial cells in PE (Figure 2D and E) and immunofluorescence analysis likewise indicated the increased expression

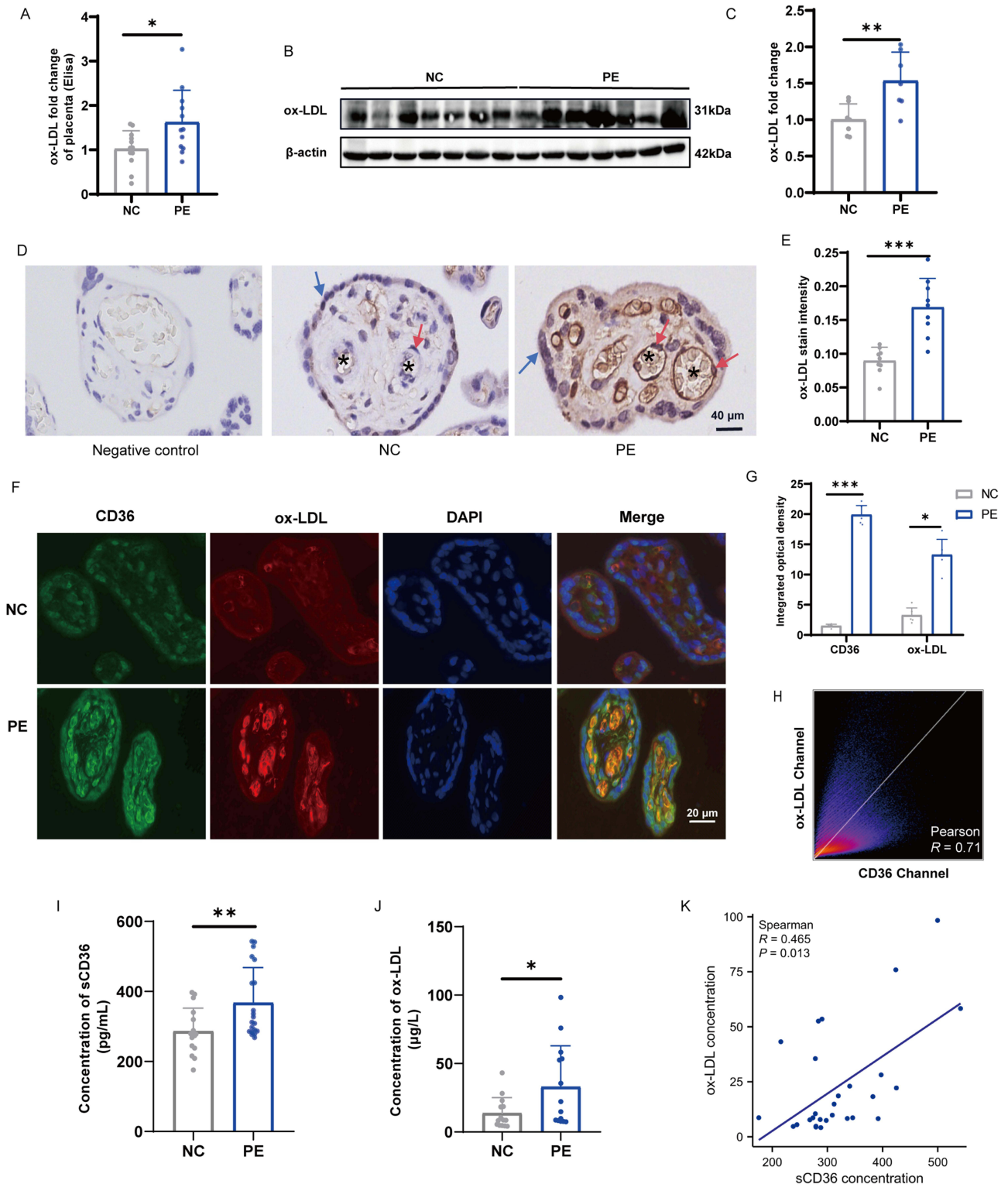

Figure 2 Ox-LDL and CD36 were significantly colocalized in the PE placenta. (**A**) Result of Elisa analysis shows the protein expression of ox-LDL in PE (n=12) and NC group (n=12); unpaired *t* test. (**B** and **C**) Western blot shows the protein expression of ox-LDL (**B**) and quantitative results in PE (n=7) and NC group (n=7) (C); unpaired *t* test. (**D** and **E**) Immunohistochemical localization of the ox-LDL (* shows the vascular lumen in the villi; red arrows show vascular endothelial cells; blue arrows show syncytiotrophoblast) (**D**) and quantitative results in PE (n=3) and NC group (n=3) (E); unpaired *t* test. (**F** and **G**) The immunofluorescence staining of CD36 (green immunofluorescence), ox-LDL (red immunofluorescence), DAPI (blue immunofluorescence) and merged (**F**) and quantitative results in PE (n=3) and NC group (n=3) (G); unpaired *t* test. (**H**) Scatter plot showing the co-expression between CD36 and ox-LDL. (**I** and **J**) Plasma sCD36 in PE (n=19) and NC group (n=16) (**I**) and ox-LDL (**J**) levels in the PE (n=14) and NC group (n=14). (**K**) Correlation between plasma sCD36 and ox-LDL levels (n=28). The data are expressed as the mean ± SD of three independent experiments; *p < 0.05, **p < 0.01, ***p < 0.001.

https://doi.org/10.2147/JIR.S538337

of ox-LDL and CD36 (Figure 2F and G), which showed better co-localization characteristics in PE placentas (R =0.71) (Figure 2F–H). Additionally, we analyzed the concentrations of soluble CD36 and ox-LDL in the plasma. Both of them exhibited elevated levels and demonstrated trends analogous to those observed in the placenta (Figure 2I–K), which suggested their potential utility as circulatory markers of PE.

PE Placentas Showed Significant Senescence-Related Phenotypes

CD36 is an important gene mediating cellular senescence, and ox-LDL has been shown to induce oxidative stress in cells, we examined the protein expression levels of key markers of cell senescence, including CDKN2A, CDKN1A, and TP53. Cellular senescence generally causes the activation of some paracrine effects. Prominent among these are inflammatory mediators, including IL-6, CXCL-8, and TNF-α, commonly elevated when senescence occurs. Therefore, we detected the protein expression levels of these inflammatory factors in placentas as well. We found that the expression of senescence markers CDKN2A, CDKN1A, and TP53 was upregulated in PE (Figure 3A and B), along with a corresponding increase in the secretion of inflammatory factors (Figure 3C–E). Since the changes in organ function or injury are frequently seen in circulation, we examined the level of these inflammatory factors in the plasma derived from pregnant women in the third trimester. We found these factors were present at varying degrees of high concentrations in PE patients (Figure 3F–H), which were consistent with the results in the placenta. To confirm that placental abnormal aging occurs, based on our transcriptome data, we conducted an enrichment analysis of age-related genes from the Aging Atlas, GenAge database, as well as the "SAUL_SEN_MAYO" gene set from the GSEA database. Results show a significant activation of aging-related genomes in the PE placentas (Table S7 and Figure 3I).

The Elevation of CD36 and Ox-LDL Coincide with the Senescence and Dysfunction of Vascular Endothelial Cells

CD36 is critical for maintaining vascular health and regulating vascular pathological conditions. Ox-LDL exists mainly in the circulation, causing damage and dysfunction to the vessels. Our immunohistochemical results also revealed high expression of CD36 at the vascular endothelium (Figure 1I). Therefore, to substantiate our hypothesis, a series of experiments were conducted on HUVECs. Overexpression and knockdown of CD36 in HUVECs were achieved through the utilization of expression plasmids and si-RNA, respectively. The efficacy of transfection was verified through qRT-PCR and Western blot analysis (Figure 4A–C). We incorporated ox-LDL at concentrations ranging from 0 to 200 μg/mL into the cell culture system and conducted CCK8 assays every 12 hours over 48 hours. The results indicated a gradual decline in the proliferation activity of HUVECs when exposed to ox-LDL concentrations exceeding 100 μg/mL (Figure 4D). Notably, significant reductions in cell proliferation were observed at ox-LDL concentrations of 150 μg/mL and 200 μg/mL (Figure 4D). Consequently, subsequent cell experiments were performed using an ox-LDL concentration of 150 μg/mL with a 24-hour intervention. Subsequently, HUVECs were categorized into four distinct groups: a control group, an ox-LDL treatment group, a group subjected to both CD36 overexpression and ox-LDL treatment and a group subjected to both CD36 knockdown and ox-LDL treatment. Intracellular levels of CD36 and ox-LDL, as well as the senescent markers CDKN2A, CDKN1A, and TP53, were assessed. The results indicated that ox-LDL intervention led to a significant upregulation of senescent markers. Furthermore, the expression of CD36 was found to modulate the levels of ox-LDL-induced senescence (Figure 4E). Additionally, we performed qRT-PCR to detect the expression of inflammatory factors in cells and found a significant role of CD36 in promoting ox-LDL-induced inflammatory (Figure 4F–H).

To characterize cellular senescence and functional abnormalities, we employed fluorescent labeling of the β-galactosidase antibody to monitor cell senescence (Figure 4I and J) and utilized the DCFH probe to assess oxidative stress levels within cells (Figure 4K and L). Additionally, we evaluated changes in the tube-forming ability of cells (Figure 4M and N). Our findings indicate that CD36 markedly enhances ox-LDL-induced cell senescence (Figure 4I and J), which is accompanied by a substantial increase in intracellular oxidative stress levels (Figure 4K and L) and a significant inhibition of the tubular formation capability of endothelial cells (Figure 4M and N).

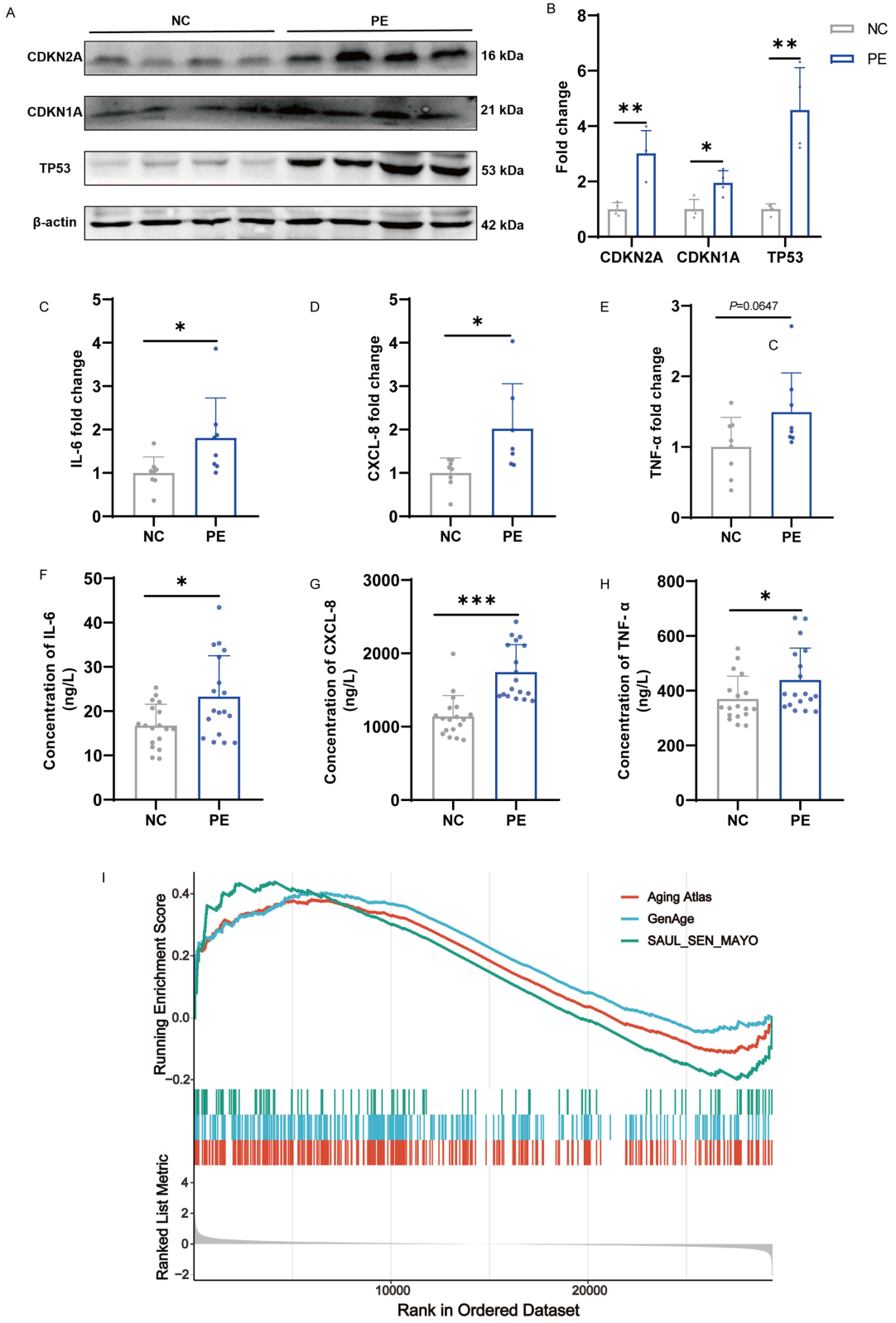

Figure 3 PE placentas showed significant senescence-related phenotypes. (**A** and **B**) Western blot analysis of CDKN2A, CDKN1A, and TP53 protein expression in PE (n=4) and NC groups (n=4) (**A**) and quantitative results (B); unpaired *t* test. (**C**–**E**) Detecting protein expression level of inflammatory factors in the PE (n=8) and NC placentas (n=8) by Elisa, including IL-6 (C), CXCL-8 (**D**) and TNF-α (E); unpaired *t* test. (**G**–**I**) Maternal plasma IL-6 (F), CXCL-8 (**G**) and TNF-α (**H**) levels in the NC (n=18) and PE group (n=18); unpaired *t* test. (**I**) Result of GSEA. Three senescence-related gene sets were significantly activated in the PE placenta (P-value < 0.05, FDR q-value < 0.25). The data are expressed as the mean ± SD of three independent experiments; *p < 0.05, **p < 0.01, ***p < 0.001.

https://doi.org/10.2147/JIR.S538337

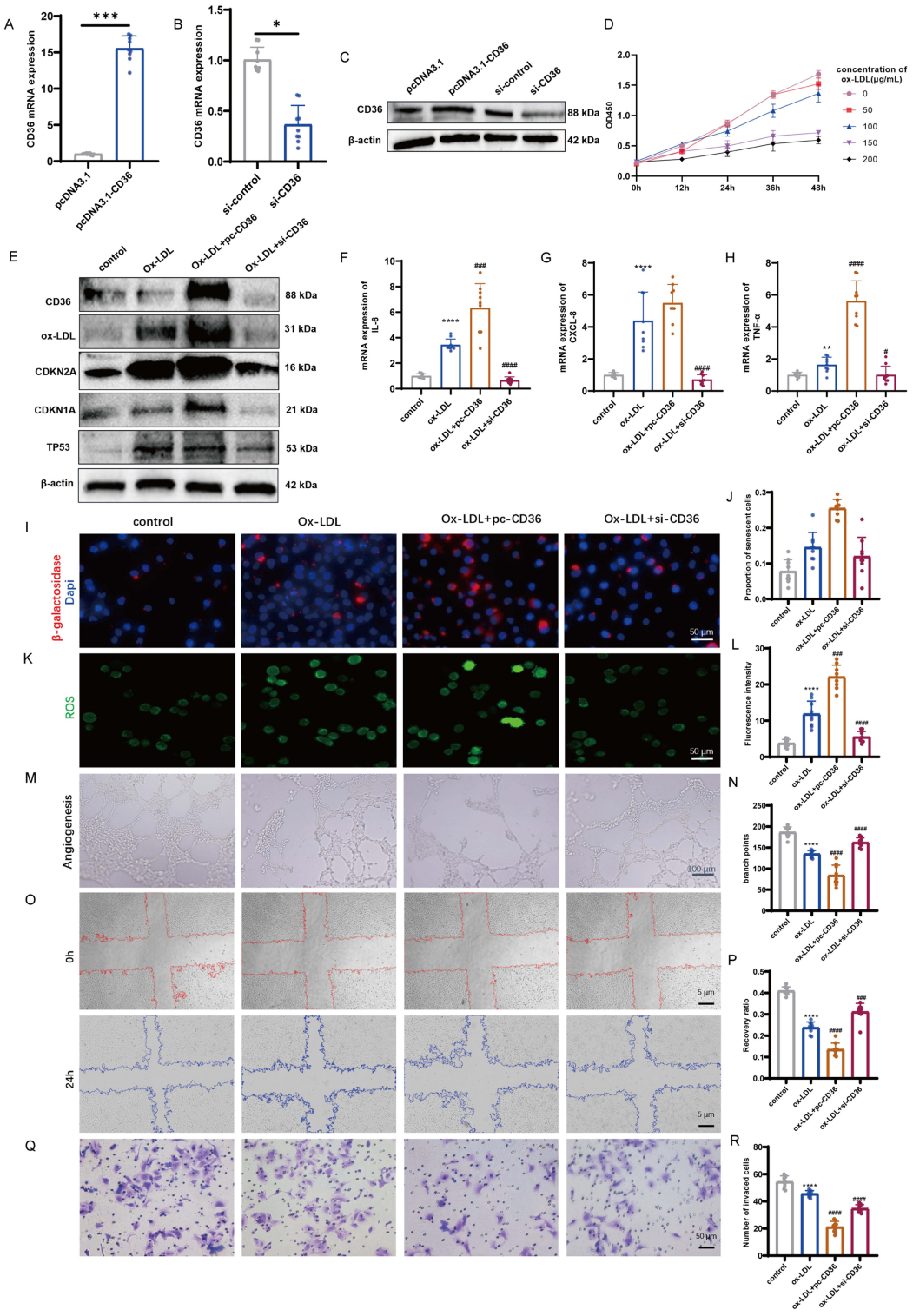

Figure 4 The Elevation of CD36 and Ox-LDL Coincide with the Senescence and Dysfunction of Vascular Endothelial Cells. (**A** and **B**) CD36 overexpression (**A**) and knockdown efficiency (**B**) in pcDNA3.1 (n=9), pcDNA3.1-CD36 (n=9), si-control (n=9) and si-CD36 (n=9) detected by qRT-PCR; unpaired *t* test. (**C**) Verification of CD36 overexpression or knockdown in HUVEC cells by Western blot. (**D**) CCK-8 analysis showed changes in cell proliferation levels after intervention with different concentrations of ox-LDL. (**E**) Western blot analysis explores the impact of CD36 expression on oxLDL-treated HUVECs. (**F** and **H**) The impact of CD36 expression on the inflammatory factors of oxLDL-treated HUVECs (n=9); *LSD-t* test. (**I** and **J**) Immunofluorescence staining of β-galactosidase showed changes in the level of cell senescence (red immunofluorescence) (**I**) and quantitative results (**J**) (n=9); *LSD-t* test. (**K** and **L**) The intracellular ROS level was measured by DCFH (green fluorescence) (**K**) and quantitative results (**L**) (n=9); *LSD-t* test. (**M** and **N**) The angiogenesis capacity of HUVECs detected by tube formation assays (**M**) and quantitative results (**N**) (n=9); *LSD-t* test. (**O** and **P**) The migration ability of HTR8/SVneo detected by scratch testing (**O**) and quantitative results (**P**) (n=9); *LSD-t* test. (**Q** and **R**) The cell invasion ability of HTR8/SVneo detected by transwell invasion assay (**Q**) and quantitative results (**R**) (n=9); *LSD-t* test. The data are expressed as the mean ± SD of three independent experiments; *p < 0.05, ***p < 0.001, ****p < 0.000; #p < 0.05, ###p < 0.001, #####p < 0.000; The calculation of * is obtained by comparing with the control group, and the # is obtained by comparing with the ox-LDL group.

Senescent cells intend to influence the surrounding tissue microenvironment via the paracrine effect, which is implicated in widespread inflammation and tissue damage. The placental trophoblast constitutes the primary cell type of the placenta. To investigate the impact of endothelial cell senescence on trophoblast function, we cultured HTR8/SVneo cells in conditioned media derived from four distinct groups of HUVEC. Subsequently, we assessed the migration (Figure 4O and P) and invasion (Figure 4Q and R) capabilities of the HTR8/SVneo cells. Our findings indicated that the secretomes generated by ox-LDL-treated endothelial cells inhibited the migration and invasion of trophoblasts and such inhibitory effect was contingent upon the expression level of CD36 in the endothelial cells (Figure 4O–R).

Discussion

There is a hormonal influence on the maternal lipid metabolism during pregnancy, so as to meet the energy metabolism and nutritional demands of the growing fetus and the construction of the placenta.[31] Lipid metabolism is closely related to the placenta, which is a vital organ during pregnancy that connects the mother and fetus. Previous studies have indicated a correlation between various pregnancy complications and disruptions in placental lipid metabolism. For instance, disturbances in lipid metabolism can affect the secretion of hormones from adipose tissue, thus interfering with insulin signaling and blood glucose regulation, leading to the onset of gestational diabetes.[32] Additionally, abnormal lipid metabolism may contribute to accelerated fetal fat synthesis and storage, as well as the ability to uptake and transport lipids, thereby increasing the risk of fetal macrosomia.[33] Although research has confirmed the presence of abnormal blood lipid levels in pregnant women with PE,[34,35] the relationship between PE and lipid metabolism abnormalities remains uncertain. Therefore, in our study, we focus on the sequencing data of the placenta. Through GSEA analysis of differentially expressed genes, we observed relatively more prominent changes in PE lipid metabolism, suggesting that lipid metabolism alterations also exist within the placenta of PE patients.

Cell senescence refers to the state of cells entering a state of permanent growth arrest and is involved in important processes such as embryonic development, aging, and wound healing.[36] It can result in the secretion of a variety of cell factors, inflammatory factors, chemokines, and matrix remodeling factors, collectively known as the SASP. The SASP is implicated in connecting cell senescence with tissue dysfunction, as it induces inflammation and cellular damage in both the senescent cells and the neighboring tissues through autocrine and paracrine mechanisms.[37] Placental aging is a normal physiological phenomenon that occurs with the progression of pregnancy. However, abnormal placental aging has been observed in patients with PE, recurrent pregnancy loss, and preterm delivery.[38] It has been found that compared to normal pregnant women, patients with PE exhibit accelerated epigenetic aging and upregulation of SASP factors in their blood and adipose tissues.[10] In the trophoblasts of the PE placenta, there is a significant trend of telomere shortening.[39] These studies suggest a close association between the onset of PE and cell senescence. In our study, we validated abnormal placental aging in patients with PE by detecting key markers of senescence and inflammatory factors involved in SASP in their placenta. These inflammatory factors are widely distributed in circulation and may be associated with the multi-organ and multi-system damage observed in PE.

The human CD36 gene is located on chromosome 7q11.2 and is one of the key proteins involved in fatty acid transport. In this signal cascade, lipids are taken up from the extracellular environment via this receptor.[13] In tumors, increased fatty acid uptake mediated by CD36 can drive tumor progression and metastasis. For instance, tumor cells promote colorectal cancer metastasis through the interaction of CD36 with fibroblasts and their lipid metabolism.[40] Palmitic acid or a high-fat diet specifically enhances the metastatic potential of CD36-positive cancer stem cells through a CD36-dependent mechanism, distinguishing them from other tumor cells based on CD36 activity and dependence on lipid metabolism.[40] CD36 has also been identified as a potential target for regulating cell senescence, and targeting this specific gene can improve muscle regeneration in mice while reducing inflammation and fibrosis occurrence.[19] As a vascular-related disease specific to pregnancy, the association among CD36, senescence, and PE has not been clarified. However, CD36 has been proven to be a functional protein molecule in PE. CD36 interacts with up-regulated THBS1 and mediated cAMP pathway to inhibit the fusion of cytotrophoblast cells, impairing placental formation and contributing to the development of PE.[40] Our study has identified CD36 as a key differentially expressed gene that appears to be involved in the development of PE based on our observations. Referring to previous research on CD36, we hypothesize from our data that CD36 might induce cell senescence, which could potentially lead to vascular dysfunction in the placenta. Our study showed an association between changes in CD36 expression and the degree of senescence in HUVECs. It was observed that these alterations in HUVEC senescence seemed to result in changes in vascular morphogenesis and function.

The role of CD36 in various cardiovascular-related diseases, particularly atherosclerosis and ischemia-reperfusion injury, should not be neglected. Available evidence has shown that soluble CD36 in serum is a component of circulating microparticles and may serve as a predictive factor for cardiovascular diseases.[41] Although there is currently no direct evidence to prove that sCD36 can serve as a predictive factor for PE, fatty acid-binding protein 4 (FABP4), a protein that acts synergistically with CD36, has been confirmed to have a predictive ability for PE when expressed at higher levels in early pregnancy.[26] We investigated whether CD36 expression varied across pre-eclampsia subtypes but found no significant differences. Instead, distinct CD36 levels were associated with FGR, LBW, and fetal sex distribution. These may indicate that up-regulated placental CD36 is a common feature among PE pregnancies rather than subtype-specific. The propensity of CD36 to drive vascular injury and senescence thereby impairs placental nutrient transport efficiency, ultimately compromising fetal growth. Our study also observed an increase in plasma sCD36 levels in patients with PE. However, due to the small sample size and the late sampling time, we are unable to confirm the diagnostic efficacy of sCD36 for PE. Nonetheless, it is plausible that CD36 may possess latent research value, both in the context of comprehending the disease mechanisms and in the realm of diagnosis and treatment for PE.

Ox-LDL is a product of low-density lipoprotein (LDL) oxidation by reactive oxygen species (ROS) and is a key lipid that induces endoplasmic reticulum stress and endothelial dysfunction.[42] Previous studies have shown that extracellular vesicles derived from the PE placenta impair endothelium-dependent vasodilation through the binding of ox-LDL to the LOX-1 receptor, leading to vascular dysfunction.[43] In our study, we detected the abnormal formation of ox-LDL in PE, prompting an investigation into the potential relationship between CD36 expression and endothelial cell senescence or damage. Our findings suggest that alterations in CD36 expression are associated with ox-LDL-induced cell senescence and angiogenesis disorders. Simultaneously, we observed alterations in intracellular oxidative stress. Given that both ox-LDL and ROS are associated with mitochondria and there are mitochondrial function changes in PE,[43] and considering that mitochondrial function alteration has been verified to be related to senescence.[43] The alteration of mitochondrial function could be a promising research avenue.

It is important to note that while our study has observed correlations between CD36 and ox-LDL expression and cell senescence, these associations remain independent observations based on a quite limited sample size rather than causative mechanisms. Senescence influenced by CD36 is more likely to be one of the factors contributing to placental senescence since the causes of abnormal placental senescence involve complex biological processes that have not yet been elucidated in PE. Our study remains preliminary findings, and it is necessary to further expand the sample size to verify the current conclusions. Besides, future research is also needed to clarify the causal relationships and underlying mechanisms among ox - LDL, CD36, and senescence in the context of PE.

Conclusion

In summary, our findings suggest that the upregulation of CD36 in vascular endothelial cells of PE placentas is associated with the increased intracellular accumulation of ox-LDL. This accumulation is accompanied by oxidative stress, secretion of inflammatory factors, and cellular senescence, which may finally impair vascular function. These injuries can locally accumulate within the placenta, leading to diminished migration and invasion capabilities of trophoblasts. The changes may eventually traverse the placental barrier and enter the systemic circulation, ultimately contributing to systemic inflammation in PE patients (Scheme 1).

Funding

This research was funded in part by the National Key Research and Development Program of China (Grant No. 2022YFC2704504), the National Natural Science Foundation of China (Grant No. 82101787, No. 82271709), the Natural Science Foundation of Guangdong Province (Grant No. 2023A1515010354, No. 2023A1515010207).

Disclosure

The authors report no conflicts of interest in this work.

References

1. Phipps E, Prasanna D, Brima W, Jim B. Preeclampsia: updates in Pathogenesis, Definitions, and Guidelines. *Clin J Am Soc Nephrol*. 2016;11(6):1102–1113. doi:10.2215/CJN.12081115
2. Murthi P, Brennecke SP. The placenta is the villain or victim in the pathogenesis of pre-eclampsia: FOR: the placenta is the villain in the pathogenesis of preeclampsia. *BJOG*. 2021;128(2):147. doi:10.1111/1471-0528.16537
3. Poon LC, Shennan A, Hyett JA, et al. The International Federation of Gynecology and Obstetrics (FIGO) initiative on pre-eclampsia: a pragmatic guide for first-trimester screening and prevention. *Int J Gynaecol Obstet*. 2019;145 Suppl(Suppl 1):1–33. doi:10.1002/ijgo.12802
4. Magee LA, Nicolaides KH, von Dadelszen P. Preeclampsia. *N Engl J Med*. 2022;386(19):1817–1832. doi:10.1056/NEJMra2109523
5. Rana S, Lemoine E, Granger JP, Karumanchi SA. Preeclampsia: pathophysiology, Challenges, and Perspectives. *Circ Res*. 2019;124(7):1094–1112. doi:10.1161/CIRCRESAHA.118.313276
6. van Deursen JM. The role of senescent cells in ageing. *Nature*. 2014;509(7501):439–446. doi:10.1038/nature13193
7. Goldman-Wohl D, Yagel S. United we stand not dividing: the syncytiotrophoblast and cell senescence. *Placenta*. 2014;35(6):341–344. doi:10.1016/j.placenta.2014.03.012
8. Sultana Z, Qiao Y, Maiti K, Smith R. Involvement of oxidative stress in placental dysfunction, the pathophysiology of fetal death and pregnancy disorders. *Reproduction*. 2023;166(2):R25–R38. doi:10.1530/REP-22-0278
9. Suvakov S, Kattah AG, Gojkovic T, et al. Impact of Aging and Cellular Senescence in the Pathophysiology of Preeclampsia. *Compr Physiol*. 2023;13(4):5077–5114. doi:10.1002/cphy.c230003
10. Suvakov S, Ghamrawi R, Cubro H, et al. Epigenetic and senescence markers indicate an accelerated ageing-like state in women with preeclamptic pregnancies. *EBioMedicine*. 2021;70:103536. doi:10.1016/j.ebiom.2021.103536
11. Londero AP, Orsaria M, Marzinotto S, et al. Placental aging and oxidation damage in a tissue micro-array model: an immunohistochemistry study. *Histochem Cell Biol*. 2016;146(2):191–204. doi:10.1007/s00418-016-1435-6
12. Qi H, Xiong L, Tong C. Aging of the placenta. *Aging*. 2022;14(13):5294–5295. doi:10.18632/aging.204175
13. Shu H, Peng Y, Hang W, Nie J, Zhou N, Wang DW. The role of CD36 in cardiovascular disease. *Cardiovasc Res*. 2022;118(1):115–129. doi:10.1093/cvr/cvaa319
14. Zhang R, Ling X, Guo X, Ding Z. CD36 Induces Inflammation by Promoting Ferroptosis in Pancreas, Epididymal Adipose Tissue, and Adipose Tissue Macrophages in Obesity-Related Severe Acute Pancreatitis. *Int J Mol Sci*. 2025;26(8):3482. doi:10.3390/ijms26083482
15. Niu H, Ren X, Tan E, et al. CD36 deletion ameliorates diabetic kidney disease by restoring fatty acid oxidation and improving mitochondrial function. *Ren Fail*. 2023;45(2):2292753. doi:10.1080/0886022X.2023.2292753
16. Zhang Y, Dong D, Xu X, et al. Oxidized high-density lipoprotein promotes CD36 palmitoylation and increases lipid uptake in macrophages. *J Biol Chem*. 2022;298(6):102000. doi:10.1016/j.jbc.2022.102000
17. Luse MA, Schug WJ, Dunaway LS, et al. Nitrosation of CD36 Regulates Endothelial Function and Serum Lipids. *Arterioscler Thromb Vasc Biol*. 2025;45(7):1067–1086. doi:10.1161/ATVBAHA.124.321964
18. Li X, Wang J, Wang L, et al. Lipid metabolism dysfunction induced by age-dependent DNA methylation accelerates aging. *Signal Transduct Target Ther*. 2022;7(1):162. doi:10.1038/s41392-022-00964-6
19. Moiseeva V, Cisneros A, Sica V, et al. Senescence atlas reveals an aged-like inflamed niche that blunts muscle regeneration. *Nature*. 2023;613(7942):169–178. doi:10.1038/s41586-022-05535-x
20. Chaiworapongsa T, Chaemsaithong P, Korzeniewski SJ, Yeo L, Romero R. Pre-eclampsia part 2: prediction, prevention and management. *Nat Rev Nephrol*. 2014;10(9):531–540. doi:10.1038/nrneph.2014.103
21. Ren Z, Gao Y, Gao Y, et al. Distinct placental molecular processes associated with early-onset and late-onset preeclampsia. *Theranostics*. 2021;11(10):5028–5044. doi:10.7150/thno.56141
22. Zhang C, Jiang S, Lu Y, Yuan F. Butorphanol tartrate mitigates cellular senescence against tumor necrosis factor -alpha (TNF-alpha) in human HC-A chondrocytes. *Bioengineered*. 2022;13(3):5434–5442. doi:10.1080/21655979.2021.2024651
23. Childs BG, Baker DJ, Wijshake T, et al. Senescent intimal foam cells are deleterious at all stages of atherosclerosis. *Science*. 2016;354(6311):472–477. doi:10.1126/science.aaf6659
24. Yang L, Wang B, Guo F, et al. FFAR4 improves the senescence of tubular epithelial cells by AMPK/SirT3 signaling in acute kidney injury. *Signal Transduct Target Ther*. 2022;7(1):384. doi:10.1038/s41392-022-01254-x
25. Di Micco R, Krizhanovsky V, Baker D, d'Adda Di Fagagna F. Cellular senescence in ageing: from mechanisms to therapeutic opportunities. *Nat Rev Mol Cell Biol*. 2021;22(2):75–95. doi:10.1038/s41580-020-00314-w
26. Qiao GH, Sun XZ. Increased plasma fatty acid binding protein 4 concentration at the first prenatal visit and its relevance to preeclampsia. *Hypertens Res*. 2018;41(9):763–769. doi:10.1038/s41440-018-0064-y
27. Li X, Li C, Zhang W, Wang Y, Qian P, Huang H. Inflammation and aging: signaling pathways and intervention therapies. *Signal Transduct Target Ther*. 2023;8(1):239. doi:10.1038/s41392-023-01502-8
28. Bernardes de Jesus B, Blasco MA. Assessing cell and organ senescence biomarkers. *Circ Res*. 2012;111(1):97–109. doi:10.1161/CIRCRESAHA.111.247866
29. Kinner A, Wu W, Staudt C, Iliakis G. Gamma-H2AX in recognition and signaling of DNA double-strand breaks in the context of chromatin. *Nucleic Acids Res*. 2008;36(17):5678–5694. doi:10.1093/nar/gkn550
30. Zhang Y, Zhan Y, Liu D, Yu B. Inhibition of microRNA-183 expression resists human umbilical vascular endothelial cells injury by upregulating expression of IRS1. *Drug Deliv*. 2019;26(1):612–621. doi:10.1080/10717544.2019.1628117
31. Riskin-Mashiah S, Damti A, Younes G, Auslender R. First trimester fasting hyperglycemia as a predictor for the development of gestational diabetes mellitus. *Eur J Obstet Gynecol Reprod Biol*. 2010;152(2):163–167. doi:10.1016/j.ejogrb.2010.05.036
32. Miturski A, Geca T, Stupak A, Kwasniewski W, Semczuk-Sikora A. Influence of Pre-Pregnancy Obesity on Carbohydrate and Lipid Metabolism with Selected Adipokines in the Maternal and Fetal Compartment. *Nutrients*. 2023;15(9):2130. doi:10.3390/nu15092130
33. Yang H, He B, Yallampalli C, Gao H. Fetal macrosomia in a Hispanic/Latinx predominant cohort and altered expressions of genes related to placental lipid transport and metabolism. *Int J Obes Lond*. 2020;44(8):1743–1752. doi:10.1038/s41366-020-0610-y

34. Szczuko M, Kikut J, Komorniak N, Bilicki J, Celewicz Z, Zietek M. The Role of Arachidonic and Linoleic Acid Derivatives in Pathological Pregnancies and the Human Reproduction Process. *Int J Mol Sci*. 2020;21(24):9628. doi:10.3390/ijms21249628
35. Mauro AK, Rengarajan A, Albright C, Boeldt DS. Fatty acids in normal and pathological pregnancies. *Mol Cell Endocrinol*. 2022;539:111466. doi:10.1016/j.mce.2021.111466
36. Wang L, Lankhorst L, Bernards R. Exploiting senescence for the treatment of cancer. *Nat Rev Cancer*. 2022;22(6):340–355. doi:10.1038/s41568-022-00450-9
37. Mehdizadeh M, Aguilar M, Thorin E, Ferbeyre G, Nattel S. The role of cellular senescence in cardiac disease: basic biology and clinical relevance. *Nat Rev Cardiol*. 2022;19(4):250–264. doi:10.1038/s41569-021-00624-2
38. Sultana Z, Maiti K, Dedman L, Smith R. Is there a role for placental senescence in the genesis of obstetric complications and fetal growth restriction? *Am J Obstet Gynecol*. 2018;218(2S):S762–S773. doi:10.1016/j.ajog.2017.11.567
39. Kohlrausch FB, Keefe DL. Telomere erosion as a placental clock: from placental pathologies to adverse pregnancy outcomes. *Placenta*. 2020;97:101–107. doi:10.1016/j.placenta.2020.06.022
40. Gong J, Lin Y, Zhang H, et al. Reprogramming of lipid metabolism in cancer-associated fibroblasts potentiates migration of colorectal cancer cells. *Cell Death Dis*. 2020;11(4):267. doi:10.1038/s41419-020-2434-z
41. Bhattacharya A, Ashouri R, Fangman M, Mazur A, Garett T, Dore S. Soluble Receptors Affecting Stroke Outcomes: potential Biomarkers and Therapeutic Tools. *Int J Mol Sci*. 2021;22(3):1108. doi:10.3390/ijms22031108
42. Nasoni MG, Crinelli R, Iuliano L, Luchetti F. When nitrosative stress hits the endoplasmic reticulum: possible implications in oxLDL/oxysterols-induced endothelial dysfunction. *Free Radic Biol Med*. 2023;208:178–185. doi:10.1016/j.freeradbiomed.2023.08.008
43. Villalobos-Labra R, Liu R, Spaans F, et al. Placenta-Derived Extracellular Vesicles From Preeclamptic Pregnancies Impair Vascular Endothelial Function via Lectin-Like Oxidized LDL Receptor-1. *Hypertension*. 2023;80(10):2226–2238. doi:10.1161/HYPERTENSIONAHA.123.21205